Journal of Signal Processing, Vol.24, No.1, pp.1-9, January 2020

PAPER

Applications and Oscillatory Phenomena of Cellular Neural Network Using Two Kinds of Cloning Templates

Yasuteru Hosokawa[1] and Yoshifumi Nishio[2]

[1]Department of Media and Information Systems, Shikoku University, 123-1 Furukawa, Ohjin, Tokushima 771-1192, Japan
[2]Department of Electrical and Electronic Engineering, Tokushima University, 2-1 Minami-Josanjima, Tokushima 770-8506, Japan
E-mail: hosokawa@keiei.shikoku-u.ac.jp, nishio@ee.tokushima-u.ac.jp

Abstract **In this paper, a cellular neural network using two kinds of cloning templates, which is a kind of modified cellular neural networks (CNN), is proposed and investigated. The structure of this system is almost the same as that of the conventional CNN. Namely, the only difference between the conventional CNN and the proposed system is the number of signal lines used for cloning templates. Therefore, the difficulty of IC implementation is almost the same. This system can carry out more complicated processing than the conventional CNN. Additionally, cloning templates of the conventional CNN can be applied to this system. As applications, five different cloning templates for image processing that can carry out complicated processing and a demonstration of an image-processing application are shown. In the demonstration, by using two cloning templates for the proposed system and three cloning templates for the conventional CNN, we demonstrate the extraction of numbers drawn with a hard-to-distinguish color in the background of postage stamps. On the other hand, oscillatory phenomena can be observed in the case of a periodic boundary condition and a symmetry-cloning template. In the case of the conventional CNN with a corresponding condition, oscillatory phenomena cannot be observed. The proposed system consists of two kinds of cells that cannot oscillate on their own. Namely, elements of the oscillator are shared among each other. In this point, the proposed system is of interest. Synchronization, quasi-synchronization and clustering phenomena are observed in the proposed system. The system is analyzed and the oscillation of the system is verified.**

Keywords: cellular neural network, nonlinear system, oscillation, coupled system

1. Introduction

The cellular neural network (CNN) was introduced by Chua and Yang [1] in 1988. This system is a kind of analog computer and its processing is faster than that of a von Neumann computer. The system can process many items of information in real time and its architecture is similar to that of a retina. Therefore, its main application is image processing [2] [3]. Many cloning templates, which determine the characteristics of the system, have been proposed. Combining these cloning templates can realize useful applications [4]-[8]. To realize applications, IC implementation is needed. Fortunately, the system consists of a regular array of the same cells, and this architecture is suitable for IC implementation [9]-[11].

On the other hand, many kinds of modified CNNs have been proposed. For instance, the delayed cellular neural network [12], fussy cellular neural network [13], quantum cellular neural network [14], small-world cellular neural network [15], shunting inhibitory cellular neural network [16] and two-layer cellular neural network [17] [18] have been proposed. Basically, these modified CNNs can carry out more complicated processing than the conventional CNN. To perform image processing using these CNNs, many processes are needed. Thus, in recent studies, the development of novel architectures applying novel semiconducting devices [19]-[21] has been addressed. However, these architectures are more complicated than that of the conventional CNN. Therefore, the advantage of the ease of IC implementation is lost.

In this paper, a cellular neural network using two kinds of cloning templates (two-template CNN) is proposed and analyzed. The only difference in the architecture between the conventional CNN and the proposed CNN is the number of signal lines used for cloning templates. Therefore, the advantage of IC implementation is not lost. The main feature of this system is that it performs more complicated processing in spite of having almost the same architecture as the conventional CNN. Furthermore, cloning templates of the conventional CNN can also be applied to this system. The proposed system can also be utilized as a conventional CNN. Hence, the advantage of the proposed system is that it has both unique characteristics and those of a conventional CNN. By demonstrating the unique characteristics of the proposed system, its effectiveness can be shown.

Five different cloning templates for image processing using the two-template CNN are proposed. These cloning templates can carry out complicated processing that cannot be carried out by the single cloning template of the conventional CNN. Four of the proposed cloning templates generate checkered patterns, from which one cloning template is proposed for the extraction of checkered patterns. Using these cloning templates, we show that one cloning template for the two-template CNN can perform more complicated processing than one cloning template for the conventional CNN.

Additionally, by using two cloning templates for the proposed system and three cloning templates for the conventional CNN, we demonstrate the extraction of numbers drawn with a hard-to-distinguish color in the background of postage stamps. The proposed system has the advantages of the ability to perform complicated processing and the flexibility of using cloning templates of the conventional CNN. This demonstration shows the superiority and the flexibility of the two-template CNN.

Another feature is that oscillatory phenomena can be observed when setting symmetry-cloning templates and a periodic boundary condition. In the case of the conventional CNN with symmetry-cloning templates and a periodic boundary condition, oscillatory phenomena cannot be observed. However, by investigating this condition, synchronization, quasi-synchronization and clustering phenomena are observed in the proposed system. This result shows that this is a novel coupled oscillatory system. This system has the feature that elements used for the oscillation are shared among each other in this system. To verify the existence of oscillatory phenomena under this condition, the case of four coupled cells is analyzed.

In Sect. 2, the architecture of the system is introduced. In Sect. 3, five different cloning templates for image processing using two-template CNN are proposed. Additionally, a demonstration of image-processing application is shown. In Sect. 4, synchronization, quasi-synchronization and clustering phenomena are shown. These phenomena are observed when setting symmetry-cloning templates and a periodic boundary condition. Additionally, the case of four coupled cells is analyzed and the existence of oscillatory phenomena is verified. Finally, conclusions are given.

2. Two-Template CNN

2.1 Architecture

Figure 1 shows the system model of the two-template CNN. We assume that the system has a two-dimensional M by N array structure. Each cell in the array is denoted as $c(i, j)$, where (i, j) is the position of the cell, $1 \leq i \leq M$ and $1 \leq j \leq N$. The coupling radius is assumed to be one.

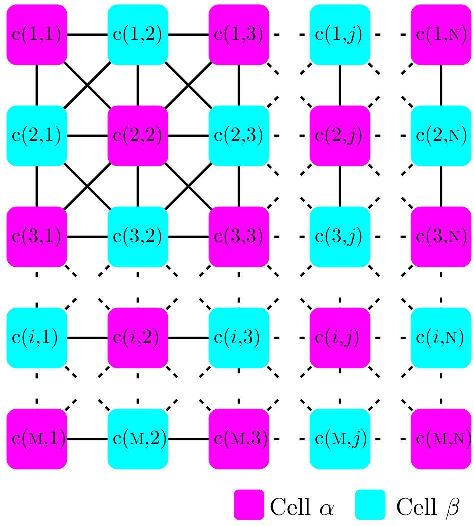

Fig. 1 System model of two-template CNN

Cells having one cloning template are called cell α and the other cells are called cell β. These two types of cells are placed as a checkered pattern, as shown in Fig. 1.

The only difference between the conventional CNN and the proposed system is the number of signal lines used for cloning templates. Therefore, the proposed system is suitable for IC implementation, similarly to the conventional CNN.

2.2 Continuous-time version

In the continuous-time version of the two-template CNN, the state equations of the cells are given as below.

1: For cell α.

$$\begin{aligned}\frac{dx_{ij}}{dt} &= -x_{ij} + I_\alpha + \sum_{(k,l)} \boldsymbol{A}_\alpha(i,j;k,l)y_{kl} \\ &\quad + \sum_{(k,l)} \boldsymbol{B}_\alpha(i,j;k,l)u_{kl}\end{aligned} \tag{1}$$

2: For cell β.

$$\begin{aligned}\frac{dx_{ij}}{dt} &= -x_{ij} + I_\beta + \sum_{(k,l)} \boldsymbol{A}_\beta(i,j;k,l)y_{kl} \\ &\quad + \sum_{(k,l)} \boldsymbol{B}_\beta(i,j;k,l)u_{kl}\end{aligned} \tag{2}$$

$\boldsymbol{A}_{\{\alpha\beta\}}(i, j; k, l)$, $\boldsymbol{B}_{\{\alpha\beta\}}(i, j; k, l)$ and $I_{\{\alpha\beta\}}$ are called the feedback coefficient, control coefficient and bias current, respectively. The variables u, x and y are the input, state and output variables of the cell, respectively. $\boldsymbol{A}_\alpha$, $\boldsymbol{B}_\alpha$, $\boldsymbol{A}_\beta$ and $\boldsymbol{B}_\beta$ are 3×3 matrices, that can be described as, for example,

$$A_\alpha =$$

$$\begin{pmatrix} A_\alpha(i,j;i-1,j-1) & A_\alpha(i,j;i-1,j) & A_\alpha(i,j;i-1,j+1) \\ A_\alpha(i,j;i,j-1) & A_\alpha(i,j;i,j) & A_\alpha(i,j;i,j+1) \\ A_\alpha(i,j;i+1,j-1) & A_\alpha(i,j;i+1,j) & A_\alpha(i,j;i+1,j+1) \end{pmatrix} \tag{3}$$

The output equation of the cell is given as follows

$$y_{ij} = 0.5(|x_{ij}+1| - |x_{ij}-1|) \tag{4}$$

2.3 Discrete-time version

In the discrete-time version of the two-template CNN, the state equations of the cells are given as follows:

1: For cell α.

$$x_{ij}(t+1) = \sum_{(k,l)\in N_r(i,j)} A_\alpha(i,j;k,l)y_{kl}(t) \\ \sum_{(k,l)\in N_r(i,j)} B_\alpha(i,j;k,l)u_{kl} + I_\alpha \tag{5}$$

2: For cell β.

$$x_{ij}(t+1) = \sum_{(k,l)\in N_r(i,j)} A_\beta(i,j;k,l)y_{kl}(t) \\ \sum_{(k,l)\in N_r(i,j)} B_\beta(i,j;k,l)u_{kl} + I_\beta \tag{6}$$

$$y_{ij}(t) = \begin{cases} 1 & (x_{ij}(t) \geq 0) \\ -1 & (x_{ij}(t) < 0) \end{cases} \tag{7}$$

3. Image Processing

In this section, five different cloning templates for image processing are shown. The first three cloning templates are for the discrete-time version and last two are for the continuous-time version. Each processing result for each cloning template set has a stable state. Namely, transient states are not used in image processing in this paper. Generally, some cloning template sets utilize transient states or repeat the image processing of a CNN. The characteristic of the proposed system contributes to reducing the number of combinations of cloning template sets. Additionally, the proposed system can also be operated as a conventional CNN. This means that many of investigations results of conventional CNNs can be utilized in the proposed system. The potential of the proposed system for image processing is shown in this section.

3.1 Hole filling and noise reduction

This cloning template can process hole filling and noise reduction at the same time. The discrete-time version described in Sec. 2.3 is applied. The boundary condition is zero and the initial state is 1, which corresponds to black. The cloning template is set as

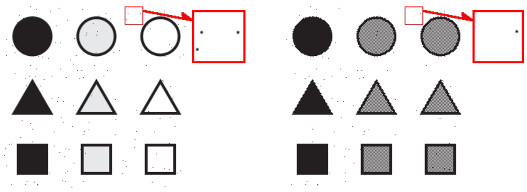

(a) (b)

Fig. 2 Computer simulation of hole filling and noise reduction: The image size is 256 × 256, (a) Input image, (b) Result

$$A_\alpha = \begin{pmatrix} 0 & 0.1 & 0 \\ 0.1 & 0 & 0.1 \\ 0 & 0.1 & 0 \end{pmatrix}, \ B_\alpha = \begin{pmatrix} 0 & 0 & 0 \\ 0 & 4 & 0 \\ 0 & 0 & 0 \end{pmatrix}, \ I_\alpha = -3.7$$
$$A_\beta = \begin{pmatrix} 1 & 0 & 1 \\ 0 & 2 & 0 \\ 1 & 0 & 1 \end{pmatrix}, \ B_\beta = \begin{pmatrix} 0 & 0 & 0 \\ 0 & 4 & 0 \\ 0 & 0 & 0 \end{pmatrix}, \ I_\beta = -0.5 \tag{8}$$

Figure 2 shows a simulation result of hole filling and noise reduction. Some black dots are removed. Center and right objects become gray areas where white and black dots are placed as a checkered pattern.

3.2 Dithering and noise reduction

This cloning template can process dithering and noise reduction at the same time. The boundary condition and initial state are the same as described in Sect. 3.1. The cloning template is set as

$$A_\alpha = \begin{pmatrix} 0 & 0.1 & 0 \\ 0.1 & 0 & 0.1 \\ 0 & 0.1 & 0 \end{pmatrix}, \ B_\alpha = \begin{pmatrix} 0 & 0 & 0 \\ 0 & 4 & 0 \\ 0 & 0 & 0 \end{pmatrix}, \ I_\alpha = -3.7$$
$$A_\beta = \begin{pmatrix} 0 & 0 & 0 \\ 0 & 0 & 0 \\ 0 & 0 & 0 \end{pmatrix}, \ B_\beta = \begin{pmatrix} -1 & -1 & -1 \\ -1 & 9 & -1 \\ -1 & -1 & -1 \end{pmatrix}, \ I_\beta = -0.5 \tag{9}$$

Figure 3 shows the simulation result of dithering and noise reduction. Some black dots are removed and the details become clear, such as the hands, camera and legs.

3.3 Edge detection

This cloning template can perform edge detection. The boundary condition and initial state are those in Sect. 3.1. The cloning template is set as

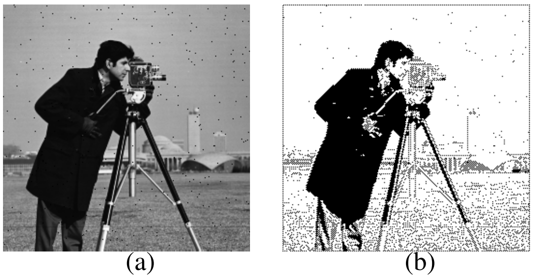

Fig. 3 Computer simulation of dithering and noise reduction: The image size is 256 × 256, (a) Input image, (b) Result

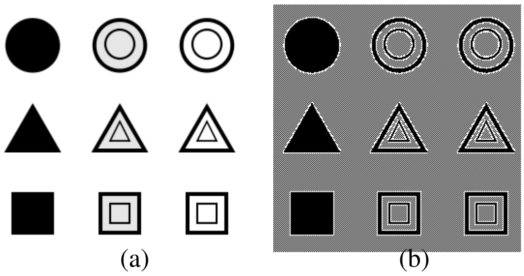

Fig. 4 Computer simulation of edge detection: The image size is 256 × 256, (a) Input image, (b) Result

$$
\begin{aligned}
&\boldsymbol{A}_\alpha = 0,\ \ \boldsymbol{B}_\alpha = \begin{pmatrix} -1 & -1 & -1 \\ -1 & 9 & -1 \\ -1 & -1 & -1 \end{pmatrix},\ \ I_\alpha = 0 \\
&\boldsymbol{A}_\beta = 0,\ \ \boldsymbol{B}_\beta = \begin{pmatrix} -1 & -1 & -1 \\ -1 & 9 & -1 \\ -1 & -1 & -1 \end{pmatrix},\ \ I_\beta = 2
\end{aligned}
\tag{10}
$$

Figure 4 shows the simulation result. Edges are detected as white. Additionally, original objects can be recognized. Gray areas are checkered patterns.

3.4 Extraction of parts with intermediate brightness

This cloning template can extract parts with intermediate brightness. The continuous-time version described in Sect. 2.2 is applied. The boundary condition is 1 and the initial state is the input image. The cloning template is set as

$$
\begin{aligned}
&\boldsymbol{A}_\alpha = \begin{pmatrix} 2 & 0 & 2 \\ 0 & 2 & 0 \\ 2 & 0 & 2 \end{pmatrix},\ \ \boldsymbol{B}_\alpha = \begin{pmatrix} 0 & 1 & 0 \\ 1 & 0 & 1 \\ 0 & 1 & 0 \end{pmatrix},\ \ I_\alpha = 2 \\
&\boldsymbol{A}_\beta = \begin{pmatrix} 2 & 1 & 2 \\ 1 & 2 & 1 \\ 2 & 1 & 2 \end{pmatrix}\ \ \boldsymbol{B}_\beta = \begin{pmatrix} -1 & -1 & -1 \\ -1 & 2 & -1 \\ -1 & -1 & -1 \end{pmatrix},\ \ I_\beta = -2
\end{aligned}
\tag{11}
$$

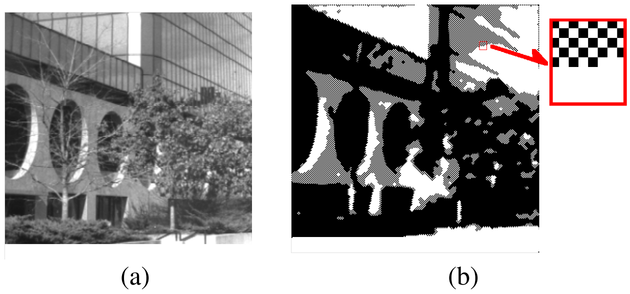

Fig. 5 Computer simulation of extraction of parts with intermediate brightness: The image size is 256 × 256, (a) Input image, (b) Result

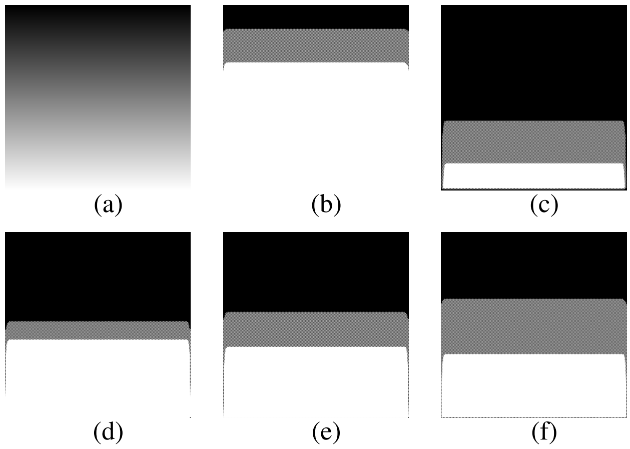

Fig. 6 Computer simulation of extraction of parts with intermediate brightness from a gradation image: The image size is 256×256, (a) Input image, (b) $I_\alpha = -5$ and $I_\beta = -6$, (c) $I_\alpha = 9$ and $I_\beta = -1$, (d) $I_\alpha = 2$ and $I_\beta = -2$, (e) $I_\alpha = 3$ and $I_\beta = -3$, (f) $I_\alpha = 4$ and $I_\beta = -4$

Figure 5 shows a simulation result of extraction of parts with intermediate brightness. By using this cloning template, parts with intermediate brightness are extracted as checkered patterns.

Changing the parameters I_α and I_β corresponds to changing the brightness and sensitivity of the extracted area. Namely, by increasing the values of I_α and I_β, the brightness of the extracted area becomes high, as shown in Figs. 6(b) and (c). By increasing the value of $I_\alpha - I_\beta$, the range of the extracted area is expanded, as shown in Figs. 6(d)-(f).

3.5 Extraction of checkered pattern

To use the proposed two-template CNN, whose output often becomes a checkered pattern, the extraction of a checkered pattern is necessary. The following cloning template can extract a checkered pattern.

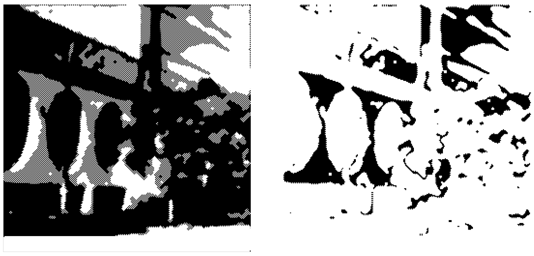

(a) (b)

Fig. 7 Computer simulation of extraction of a checkered pattern: The image size is 256 × 256, (a) Input image, (b) Result

$$\boldsymbol{A}_\alpha = 0,\ \boldsymbol{B}_\alpha = \begin{pmatrix} 1 & -1 & 1 \\ -1 & 1 & -1 \\ 1 & -1 & 1 \end{pmatrix},\ I_\alpha = -6$$
$$\boldsymbol{A}_\beta = 0,\ \boldsymbol{B}_\beta = \begin{pmatrix} -1 & 1 & -1 \\ 1 & -1 & 1 \\ -1 & 1 & -1 \end{pmatrix},\ I_\beta = -6 \tag{12}$$

Figure 7 shows a simulation result of extraction of a checkered pattern. The input image is the same as that in Fig. 5(b). The checkered pattern is extracted.

3.6 Demonstration of image-processing application

The extraction of parts with intermediate brightness can be realized by combining the cloning templates described in Sects. 3.4 and 3.5. Here, as an application, the extraction of numbers drawn with a hard-to-distinguish color in the background of postage stamps is demonstrated.

Numbers in postage stamps are an important feature of stamps. However, sometimes the numbers are drawn with a hard-to-distinguish color in the background because the design of the postage stamps is emphasized. An algorithm based on the conventional CNN for the extraction of numbers drawn with a hard-to-distinguish color has been proposed by Kishida et al. [22]. In their algorithm, six or more cloning templates are needed. Additionally, many iterations, the adjustment of some parameters or additional processing is needed for the processing of some cloning templates, and the procedure is complicated. By using the two-template CNN, a similar result can be obtained with much a simpler algorithm.

Figure 8 shows the extraction of numbers from the background of a postage stamp. Figure 8(a) shows an input image. Figure 8(b) shows an image with intermediate-brightness parts (gray areas) extracted as checkered patterns. Here, the cloning template in Eq. (11) with values changed to $I_\alpha = -1$ and $I_\beta = -2.5$ is applied. Figure 8(c) shows an image with the intermediate-brightness parts from Fig. 8(b) in black, where the cloning template in Eq. (12) was applied. By applying peel, grow and subtract

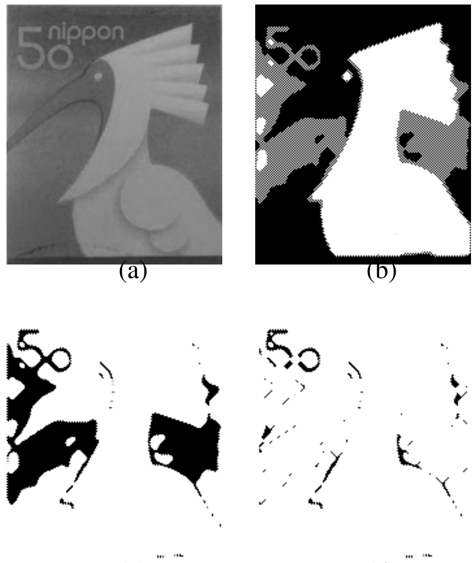

(a) (b)

(c) (d)

Fig. 8 Extraction of numbers drawn with a hard-to-distinguish color from the background of postage stamps: The image size is 166 × 200, (a) Input image, (b) Intermediate brightness parts extracted as checkered patterns, (c) Extracted intermediate-brightness parts in black, (d) Extracted numbers after removing large black areas

templates, which are the cloning templates of the conventional CNN, to Fig. 8(c), large black areas are removed. Figure 8(d) shows that the numbers are extracted.

4. Oscillatory Phenomena

In this section, some oscillatory phenomena are shown. On a conventional CNN with applied symmetrical-cloning template values, oscillatory phenomena cannot be observed. There are some modified CNNs that can generate oscillatory phenomena [23] - [24]. The intentionally modification for oscillatory phenomena is applied to these system. The proposed system is modified utilizing only two cloning template sets. The values applied to the cloning template are symmetric values. The structure of the proposed system is interesting as a coupled oscillatory system. Normally, a coupled oscillatory system consists of oscillators and coupling elements. However, the proposed system cannot be divided into oscillators and coupling elements because the elements of oscillator are shared among each other. There are no similar systems in the field of electronic oscillators. Couplied systems are classified into continuous or discrete. For instance, a system of coupled electronic oscillators is classified as a continuous-time, continuous-valued and discrete-space system. As another example, a coupled map lattice is classified as a discrete-time, continuous-valued and discrete-space system. The proposed system is not easy to classify in this way, the space cannot be classified as continuous or discrete. The interesting point of the proposed system is this structure. Some observed phenomena in the proposed system and a basic analysis of the oscillation are shown below.

4.1 Simulation settings

In this section, synchronization, quasi-synchronization and clustering phenomena are shown using the following conditions. Boundary conditions are set as periodic. Cloning templates are set as symmetrical as follows.

$$\begin{aligned} \boldsymbol{A}_\alpha &= \begin{pmatrix} -p & q & -p \\ q & r & q \\ -p & q & -p \end{pmatrix}, \ \boldsymbol{B}_\alpha = 0, \ I_\alpha = 0 \\ \boldsymbol{A}_\beta &= \begin{pmatrix} p & -q & p \\ -q & -r & -q \\ p & -q & p \end{pmatrix}, \ \boldsymbol{B}_\beta = 0 \ I_\beta = 0 \end{aligned} \tag{13}$$

The network size is 8×8. The initial state is set at random. The input values do not affect the result because $\boldsymbol{B}_\alpha = \boldsymbol{B}_\beta = 0$.

4.2 Synchronization phenomena

Figures 9(1) and (2) show synchronization phenomena. The parameters of the cloning templates are set as $p = 2$, $q = 4$ and $r = 0$. These two results are obtained from two different random initial states, as shown in Figs. 9(1)(a) and (2)(a). The two results show periodic oscillations. The phenomena shown in Figs. 9(1)(b) and (2)(b) to Figs. 9(1)(j) and (2)(j), respectively, are repeated via transient states from the initial state, as shown in Figs. 9(1)(a) and (2)(a). All cells are divided into three groups. For instance, the value of cell $c(1,1)$ in Fig. 9(1) (e) is synchronized with the value of cells $c(3,1)$, $c(1,3)$, $c(3,3)$ and so on. This group is called Cell α_1 in this study. In the same way, the cell $c(2,2)$ group is called Cell α_2. All cells β are synchronized. Therefore, this group is called Cell β. Figures 10(1) and (2) show the waveforms of Figs. 9(1) and (2), respectively. Each group is synchronized via a transient state.

A difference between the two figures is that Cell α_1 and Cell α_2 are placed on opposite sides from each other. These waves synchronize in phase. Additionally, Cells β are also synchronized. Note that all waves synchronize in phase and the offsets have different values.

4.3 Quasi-synchronization phenomena

Figure 11 shows quasi-synchronization phenomena. The parameters of the cloning templates are set as $p = 2$, $q = 3$ and $r = 0$. The waveforms are blurred. Additionally, burst parts are observed in the center part. The snapshots when this burst occurred are similar to those in Fig. 9. However, some cells are delayed temporarily. This delay is observed as the burst.

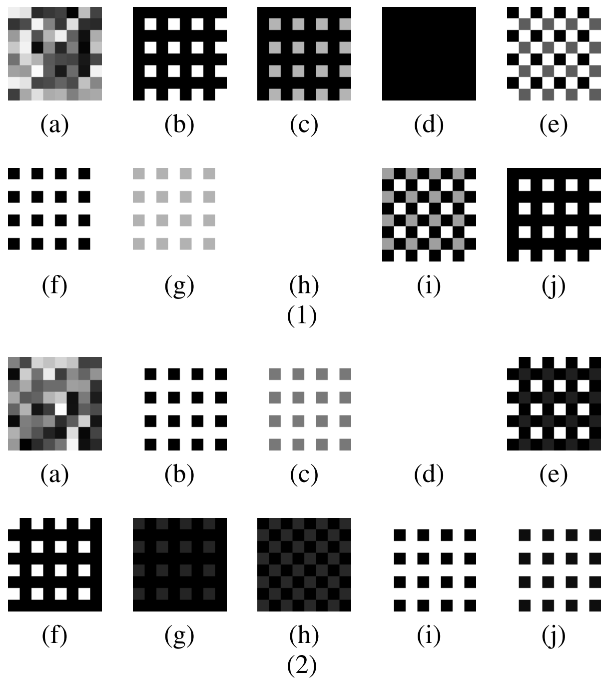

Fig. 9 Oscillatory phenomena starting from two different initial states: $p = 2$, $q = 4$, $r = 0$, (a) Initial state, (b) - (j) Snapshots, The iteration numbers of (1) are (b) 10010, (c) 10040, (d) 10070, (e) 10100, (f) 10130, (g) 10160, (h) 10190, (i) 10210 and (j) 10240, The iteration numbers of (2) are (b) 10080, (c) 10110, (d) 10140, (e) 10170, (f) 10200, (g) 10260, (h) 10290, (i) 10210 and (j) 10320

4.4 Clustering phenomena

Figure 12 shows clustering phenomenon. The parameters of the cloning templates are set as $p = 3$, $q = 4$ and $r = 1$. Depending on initial states, similar phenomena to those shown in Figs. 10 or 11 can also be observed for these parameters. The waveforms are divided into 16 clusters as shown in Fig. 12. Namely, the waveforms are divided into four, which are named Cell α_1, Cell α_2, Cell β_1 and Cell β_2, and each Cell is divided into four clusters by phases. The difference in the phases is 90 degrees per cluster. Each cluster consists of four Cells. These clusters are divided regularly. For instance, Cell $\alpha_1 - 1$ includes $c(1,1)$, $c(3,1)$, $c(5,1)$ and $c(7,1)$, Cell $\alpha_1 - 2$ includes $c(1,3)$, $c(3,3)$, $c(5,3)$ and $c(7,3)$, Cell $\alpha_1 - 3$ includes $c(1,5)$, $c(3,5)$, $c(5,5)$ and $c(7,5)$ and Cell $\alpha_1 - 4$ includes $c(1,7)$, $c(3,7)$, $c(5,7)$ and $c(7,7)$. In the four clusters of Cell α_2, Cell β_1 and Cell β_2, the same relationships are observed.

4.5 Analysis of oscillation

Normally, coupled oscillatory systems consist of oscillators and coupling elements. Namely, an oscillator can oscillate on its own. However, the proposed system consists of two kinds of cells that cannot oscillate on their

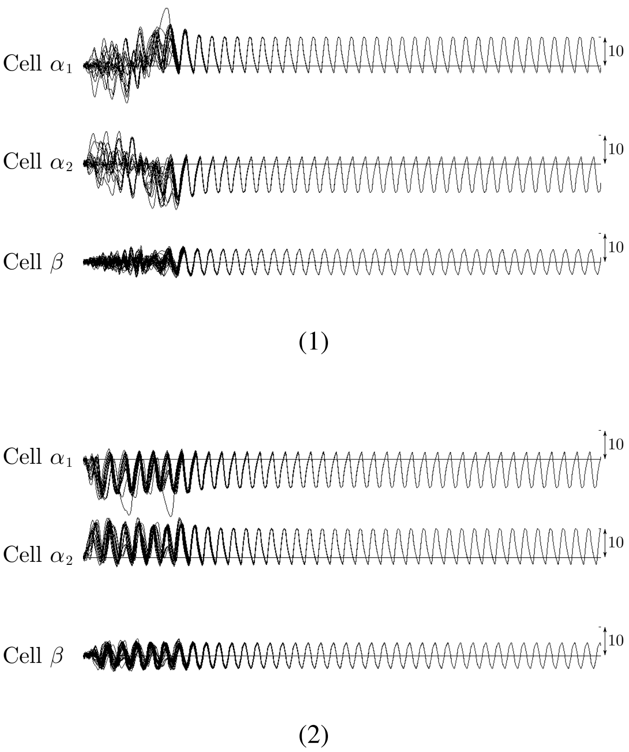

Fig. 10 Time series of oscillatory phenomena shown in Figs. 9(1) and (2)

own. The elements of the oscillator are shared among each other. Regarding this point, it is considered that the proposed system is a novel oscillatory system. Additionally, the waveforms, phases and so on of these oscillations are influenced by the positions of the cells. For instance, the results in Fig. 10 show that Cell α plays two roles in spite of it being the same kind of cell in the system. Therefore, three kinds of waveforms are observed. These phenomena can only be observed in the proposed system. Oscillatory phenomena cannot be observed in the conventional CNN with the symmetry-cloning template. The observation of oscillatory phenomena in the proposed system is also an interesting point. In this section, the mechanism of the scillation of the proposed system is verified.

In the proposed system, oscillatory phenomena can be observed easily with fixed boundary conditions. However, it is not so easy to observe oscillatory phenomena with periodic boundary conditions. The reason why it is difficult is that the states of the proposed system basically correspond to the stable state of the conventional CNN, which is mentioned in [1]. The only difference is that two kinds of templates are applied in the proposed system. Therefore, the observation of oscillatory phenomena is very interesting and it is considered that using two kinds of templates causes the oscillatory phenomena.

According to the results of many computer simulations, the minimum number of cells required to observe oscillatory phenomena is four. Namely, the simplest architecture

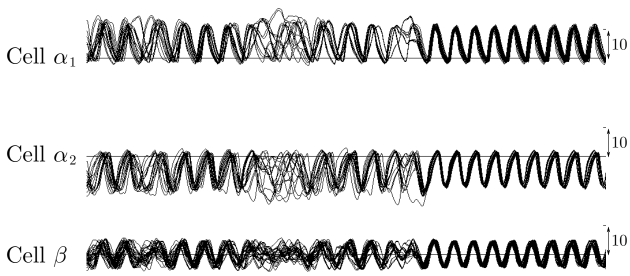

Fig. 11 Quasi-synchronization including burst parts

required for an oscillation consists of four cells. In this section, the simplest architecture shown in Fig. 13 is investigated and the mechanism of the oscillation is revealed.

The output function y_{ij} is defined as the piecewise linear function in Eq. (4). Each region is defined as follows.

$$\begin{array}{lcl} D^{+} & \equiv & \{x > 1\} \\ D^{0} & \equiv & \{1 \leq x \leq -1\} \\ D^{-} & \equiv & \{x < -1\} \end{array} \tag{14}$$

There are four cells, each with three regions. Consequently, the number of combinations is $3^4 = 81$, which is too many to analyze. Hence, the regions that the orbit pass through are investigated by computer simulation. Table 1 shows wandering of the orbit. The parameters are set to be the same as those in Fig. 9. The orbit passes through regions in numerical order. When the orbit reaches the end of No. 12, it returns to No. 1. Sometimes, Nos. 3 and 9 are skipped. The eigenvalues of these regions are derived as shown in Table 2. In region Nos. 2, 3, 8 and 9, the orbit does not converge because of the eigenvalues include a positive value. In the other regions, equilibrium points exist outside the regions, as shown in Table 3. Therefore, the orbit does not converge in these regions. These results show that the system does not oscillate in one region, and a combination of attraction to the equilibrium points of each region generates the oscillation.

According to the result of this analysis, this system can oscillate in the case of symmetry-cloning templates. In the conventional CNN, symmetry-cloning templates could not oscillate. This point is one of the important features of the two-template CNN.

5. Conclusions

In this paper, a cellular neural network using two kinds of cloning templates, which is a kind of modified cellular neural networks, has been proposed and investigated. This system can carry out more complicated processing than the conventional CNN. Additionally, cloning templates of the conventional CNN can be applied to this system. As applications, five different cloning templates for image processing that can carry out complicated processing and a demon-

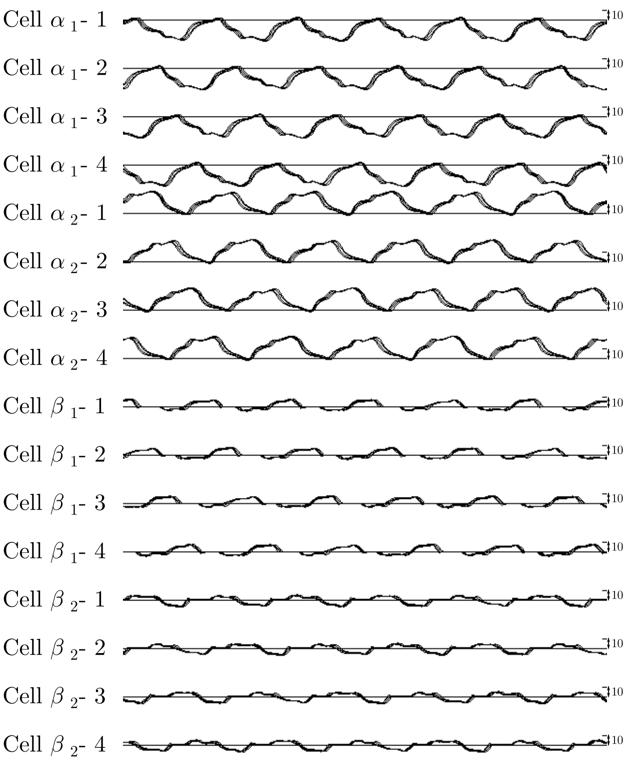

Fig. 12 Computer simulation result in which 16 clusters were observed

stration of an image-processing application were shown. On the other hand, clustering phenomena of oscillations could be observed in the case of periodic boundary condition and a symmetry-cloning template. The system was analyzed and the oscillation of the system was verified. It is considered that these results show the potencial of the two-template CNN.

Developing various new cloning templates, investigations of oscillatory phenomena and so forth, are our future works.

Acknowledgment

This work was partly supported by JSPS Grant-in-Aid for Scientific Research 16K06357.

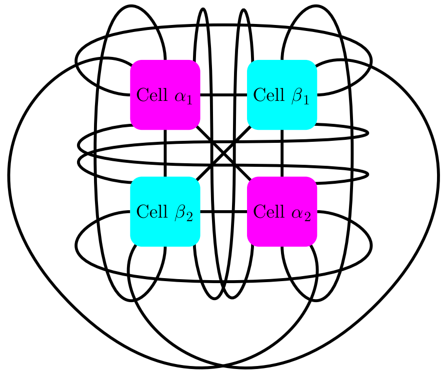

Fig. 13 Simplest architecture of two template CNN

Table 1 Wandering of the orbit

No.	Cell α_1	Cell β_1	Cell α_2	Cell β_2
1	D^-	D^-	D^-	D^-
2	D^-	D^0	D^0	D^-
3	D^-	D^0	D^0	D^0
4	D^-	D^+	D^+	D^0
5	D^-	D^+	D^+	D^+
6	D^0	D^+	D^+	D^+
7	D^+	D^+	D^+	D^+
8	D^+	D^0	D^0	D^+
9	D^0	D^0	D^0	D^+
10	D^0	D^-	D^-	D^+
11	D^-	D^-	D^-	D^+
12	D^-	D^-	D^-	D^0

References

[1] L. O. Chua and L. Yang: Cellular neural networks: Theory, IEEE Trans. Circuits and Systems, Vol.35, No.10, pp.1257-1272, 1988.

[2] L. O. Chua and L. Yang: Cellular neural networks: Applications, IEEE Trans. Circuits and Systems, Vol.35, No.10, pp.1273-1290, 1988.

[3] L. O. Chua and T. Roska: Cellular Neural Networks and Visual Computing: Foundation and Applications, Cambridge University Press, 2002.

[4] T. Matsumoto, L. O. Chua and R. Furukawa: CNN cloning template: Hole-filler, IEEE Trans. Circuits and Systems, Vol.37, No.5, pp.635-638, 1990.

[5] T. Matsumoto, L. O. Chua and R. Furukawa: CNN cloning template: shadow detector, IEEE Trans. Circuits and Systems, Vol.37, No.8, pp.1070-1073, 1990.

[6] T. Kozek, T. Roska and L. O. Chua: Genetic algorithm for CNN template learning, IEEE Trans. Circuits and Systems I, Vol.40, No.6, pp.392-402, 1993.

[7] K. R. Crounse, T. Roska and L. O. Chua: Image halftoning with cellular neural networks, IEEE Trans. Circuits and Systems II, Vol.40, No.4, pp.267-283, 1993.

[8] K. R. Crounse and L. O. Chua: Methods for image processing and pattern formation in cellular neural networks: A tutorial, IEEE Trans. Circuits and Systems I, Vol.42, No.10, pp.583-601, 1995.

[9] L. Yang, L. O. Chua and K. R. Krieg: VLSI implementation of cellular neural networks, Proc. Int. Symp. Circuits and Systems, Vol.3, pp.2425-2427, 1990.

[10] J. E. Varrientos, E. Sanchez-Sinencio and J. Ramirez-Angulo: A current-mode cellular neural network implementation, IEEE Trans. Circuits and Systems II, Vol.40, No.3, pp.147-155, 1993.

[11] G. C. Cardarilli, R. Lojacono, M. Salerno and F. Sargeni: VLSI implementation of a cellular neural network with programmable control operator, Proc. Midwest Symp. Circuits and Systems, Vol.2,

Table 2 Eigenvalues of each region

No.	Eigenvalues
1	$-1, -1, -1, -1$
2	$-1, 6, -10, -1$
3	$-1, -10, 3 \pm j7.937$
4	$-1, -1, -1, -1$
5	$-1, -1, -1, -1$
6	$-1, -1, -1, -1$
7	$-1, -1, -1, -1$
8	$-1, 6, -10, -1$
9	$-1, -10, 3 \pm j7.937$
10	$-1, -1, -1, -1$
11	$-1, -1, -1, -1$
12	$-1, -1, -1, -1$

Table 3 Equilibrium points of each region

No.	Equilibrium points ($x_{(1,1)}$, $x_{(1,2)}$,$x_{(2,1)}$, $x_{(2,2)}$)
1	$(-8, 8, 8, -8)$
4	$(8, 64, 64, 80)$
5	$(8, 8, 8, 24)$
6	$(8, -64, -64, -48)$
7	$(8, -8, -8, 8)$
10	$(8, -48, -64, -64)$
11	$(8, 24, 8, 8)$
12	$(64, 80, 8, 64)$

pp.1089-1092, 1993.

[12] T. Roska and L. O. Chua: Cellular neural networks with nonlinear and delay-type template elements, Proc. Int. Workshop on Cellular Neural Networks and Their Applications, pp.12-25, 1990.

[13] T. Yang, L. B. Yang, C. W. Wu and L. O. Chua: Fuzzy cellular neural networks: Theory, Proc. Int. Workshop on Cellular Neural Networks and Their Applications, pp.181-186, 1996.

[14] W. Porod, C. S. Lent, G. Tóth, H. Luo, A. Csurgay, Y.-F. Huang and R.-W. Liu: Quantum-dot cellular nonlinear networks: Computing with locally-connected quantum dot arrays, Proc. Int. Symp. Circuits and Systems, Vol.1, pp.745-748, 1997.

[15] K. Tsuruta, Z. Yang, Y. Nishio and A. Ushida: Small-world cellular neural networks for image processing applications, Proc. European Conf. on Circuit Theory and Design, Vol.1, pp.225-228, 2003.

[16] A. Bouzerdoum and R. B. Pinter: Shunting inhibitory cellular neural networks: Derivation and stability analysis, IEEE Trans. Circuits and Systems I, Vol.40, No.3, pp.215-221, 1993.

[17] P. Arena, S. Baglio, L. Fortuna and G. Manganaro: Complexity in a two-layer CNN, Proc. Int. Workshop Cellular Neural Networks and Their Applications, pp.127-132, 1996.

[18] Z. Yang, Y. Nishio and A. Ushida: Templates and algorithms for two-layer cellular neural networks, Proc. Int. Symp. on Nonlinear Theory and Its Applications Vol.2, pp.1946-1951, 2002.

[19] J. C. Ban, C. H. Chang and S. S. Lin: On the structure of multilayer cellular neural networks, Differential Equations, Vol.252, No.8, pp.4563-4597, 2012.

[20] J. J. Martinez, J. Garrigos, J. Toledo and J. M. Ferrandez: An efficient and expandable hardware implementation of multilayer cellular neural networks, Neurocomputing, Vol.114, pp.54-62, 2013.

[21] X. Hu, G. Feng, S. Duan and L. Liu: A memristive multilayer cellular neural network with applications to image processing, IEICE Trans. Neural Networks and Learning Systems, Vol.28, No.8, pp.1889-1901, 2017.

[22] J. Kishida, C. Rekeczky, Y. Nishio and A. Ushida: Feature extraction of postage stamps using an iterative approach of CNN, IEICE Trans. Fundamentals, Vol.E79-A, No.10, pp.1741-1746, 1996.

[23] L. O. Chua, M. Hasler, G. S. Moschytz and J. Neirynck: Autonomous cellular neural networks: A unified paradigm for pattern formation and active wave propagation, IEEE Trans. Circuits Syst. I, Vol.42, No.10, pp.559-577, 1995.

[24] A. Y. Pogromsky and H. Nijmeijer: On oscillations in cellular neural networks, Proceedings of the 38th IEEE Conference on Decision and Control, pp.2629-2634, Dec. 1999.

Yasuteru Hosokawa received his B.E., M.E. and Ph.D. degrees from Tokushima University, Tokushima Japan, in 1997, 1999 and 2002, respectively. In 2001, he joined the Faculty of Management and Information Science at Shikoku University, Tokushima, Japan, where he is currently an Associate Professor. From August 2016, he spent four months at Saginaw Valley State University (SVSU) as a Visiting Professor. His research interest is in chaotic circuit systems. He is currently the Vise Chair of the IEEE CAS Society Shikoku Chapter. He is a member of the IEICE, IEEE and RISP.

Yoshifumi Nishio received his B.E., M.E. and Ph.D. degrees in electrical engineering from Keio University, Yokohama, Japan, in 1988, 1990 and 1993, respectively. In 1993, he joined the Department of Electrical and Electronic Engineering at Tokushima University, Tokushima, Japan, where he is currently a Professor. From May 2000, he spent a year in the Laboratory of Nonlinear Systems (LANOS) at the Swiss Federal Institute of Technology Lausanne (EPFL) as a Visiting Professor. His research interests include analysis and application of chaos in electrical circuits, analysis of synchronization in coupled oscillatory circuits, development of methods for analyzing nonlinear circuits, theory and application of cellular neural networks, and neural network architecture. He was the Chair of the IEEE CAS Society Technical Committee on Nonlinear Circuits and Systems (NCAS) during 2004–2005, the Steering Committee Secretary of the IEICE Research Society of Nonlinear Theory and its Applications (NOLTA) during 2004–2007, and is currently the Secretary/Treasurer of the IEEE CAS Society Shikoku Chapter. He was an Associate Editor of IEEE Transactions on Circuits and Systems–I: Regular Papers during 2004–2005 and IEEE CAS Magazine during 2008–2009, and is currently serving as an Associate Editor for IEEE Transactions on Circuits and Systems–II: Express Briefs, the IEEE CAS Society Newsletter. He is also the Editor of NOLTA, IEICE and IEICE Fundamentals Review and a member of the Editorial Board of International Journal of Circuit Theory and Applications. He is a senior member of the IEEE and a member of IEICE and RISP.

(Received March 16, 2019; revised August 9, 2019)